Inorganic Chemistry

ARTICLE

pubs.acs.org/IC

Dimethylaminoborane (H_2BNMe_2) Coordination to Late Transition Metal Centers: Snapshots of the B−H Oxidative Addition Process

Gaëtan Bénac-Lestrille,[†,‡] Ulrike Helmstedt,[§] Laure Vendier,[†,‡] Gilles Alcaraz,*[,†,‡] Eric Clot,*[,§] and Sylviane Sabo-Etienne*[,†,‡]

[†]LCC (Laboratoire de Chimie de Coordination), CNRS, 205 Route de Narbonne, F-31077 Toulouse, France

[‡]Université de Toulouse, UPS, INPT, F-31077 Toulouse, France

[§]Institut Charles Gerhardt, CNRS 5253, Université Montpellier 2, cc 1501, Place Eugène Bataillon, 34095 Montpellier, France

Supporting Information

ABSTRACT: The reaction of cyclodiborazane $[Me_2N\text{-}BH_2]_2$ with the chloro(dihydrogen) ruthenium complex $RuHCl(\eta^2\text{-}H_2)(P^iPr_3)_2$ (**1**) led to the formation of the unsymmetricaly coordinated dimethylaminoborane complex $RuHCl(H_2BNMe_2)(P^iPr_3)_2$ (**2**). The dimethylaminoborane coordination (H_2BNMe_2) to the ruthenium center in **2** was carefully studied by combining X-ray, multinuclear NMR, and density functional theory (DFT) techniques, and compared with the recently reported osmium analogue which was originally formulated as a σ-B−H borinium complex $[OsH_2Cl(HBNMe_2)(P^iPr_3)_2]$ (**4**). All our data are in favor of a bis(σ-B−H) coordination mode at a very activated stage in the case of the ruthenium complex **2**, whereas in the osmium complex **4**, full oxidative addition is favored leading to a complex better formulated as an osmium(IV) boryl species with an α-agostic B−H interaction. The synthesis and characterization of the symmetrical dihydride complex $RuH_2(H_2BNMe_2)(P^iPr_3)_2$ (**3**) from addition of the lithium dimethylaminoborohydride to **1** is reported for comparison.

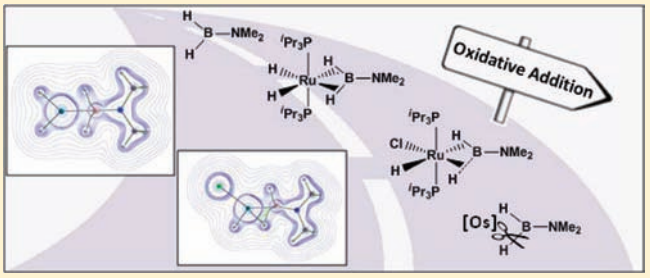

INTRODUCTION

Beyond the well-known metal-catalyzed hydroboration reaction, B−H bond activation is an extremely active research area connected both to major industrial issues and to environmental concerns. Research toward chemical hydrogen storage, production of inorganic polymers, or borylation of alkanes or arenes has attracted considerable interest and contributed to the establishment of new bonding modes as a function of the B−H bond activation level.[1] With regard to disubstituted boranes (R_2BH), the formation of hydrido boryl species in a final B−H bond activation stage is well documented. Since the isolation of the first σ-borane complex by Hartwig et al. in 1996,[2] a limited but growing number of disubstituted borane ligated transition metal complexes has been formulated as σ-borane species.[3] The coordination chemistry of monosubstituted boranes is a more recent area. In 2007, we reported an unprecedented symmetrical coordination of a monosubstituted borane (RBH_2) to a ruthenium center resulting from two geminal σ-B−H bonds in a 4-center, 4-electron interaction mode.[4] In the case of monosubstituted aminoboranes ($R_2N\text{-}BH_2$), this coordination mode was recently extended to Ru and cationic Rh and Ir centers.[5] In that case, the coordination occurred through three synthetic pathways, namely, direct coordination, retrodimerization, or even amine-borane dehydrogenation from the corresponding precursors.

In the case of the mesitylborane ($MesBH_2$) and starting from the ruthenium chloro complex $RuHCl(\eta^2\text{-}H_2)(PCy_3)_2$ (**1**), we disclosed a straightforward access to the terminal borylene complex $RuHCl(BMes)(PCy_3)_2$.[6] This reaction which enables a further activation of the two B−H bonds of the starting borane involves an intermediate that, on the basis of NMR data, we tentatively formulated as $RuHCl(\eta^2\text{:}\eta^2\text{-}H_2BMes)(PCy_3)_2$ featuring an unsymmetrical bis(σ-B−H) mesitylborane ligand. Very recently, Aldridge et al. reported two systems involving the coordination of the aminoborane (H_2BNCy_2) which are particularly relevant to the pivotal question of the B−H activation process. A mono (σ-B−H) binding mode was established upon coordination to the $[CpRu(PR_3)_2]^+$ fragment,[7] whereas the hydrido(boryl) complex $IrHCl(BHNCy_2)(PMe_3)_3$ was shown to be a precursor for the formation of the cationic borylene complex $[IrH_2(BNCy_2)(PMe_3)_3][BAr_4]$ through α-hydrogen migration.[8] More puzzling was the σ-(B−H) borinium formulation of the osmium complex $OsH_2Cl(HBNMe_2)(P^iPr_3)_2$ (**4**), as reported by Esteruelas et al.[9] This complex was obtained by addition of dimethylamine-borane to $OsH_2Cl_2(P^iPr_3)_2$.

With this in mind, and looking for additional information on the overall dihydroborane to borylene transformation process, we focused on the problem of the unsymmetrical coordination

Received: July 22, 2011
Published: September 28, 2011

dx.doi.org/10.1021/ic201573q | *Inorg. Chem.* 2011, 50, 11039–11045

Scheme 1. Synthesis of the Dimethylaminoborane Ruthenium Complexes 2 and 3

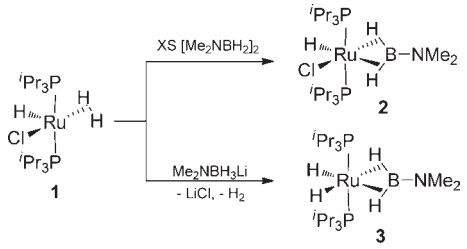

mode of RBH_2 at a metal center. We chose dimethylaminoborane as a more suitable precursor with respect to mesitylborane, to compare and elucidate the influence of the metal center on the coordination. Here, we report the synthesis and characterization of $RuHCl(H_2BNMe_2)(P^iPr_3)_2$ (**2**) and $RuH_2(H_2BNMe_2)(P^iPr_3)_2$ (**3**) and an in-depth analysis of the coordination mode of Me_2NBH_2, in particular through computational studies on the $MHX(H_2BNMe_2)(PMe_3)_2$ species (X = H, Cl; M = Ru, Os).

RESULTS AND DISCUSSION

Reaction of $RuHCl(\eta^2\text{-}H_2)(P^iPr_3)_2$ (**1**) with an excess of dimethylaminoborane dimer was carried out at room temperature for 18 h. After workup, a yellow powder analyzed as $RuHCl(H_2BNMe_2)(P^iPr_3)_2$ (**2**) was isolated (69% yield) and fully characterized by NMR and X-ray diffraction crystallography (Scheme 1). The $^{11}B\{^1H\}$ NMR spectrum in C_6D_6 shows a broad signal centered at δ 56, thus in a region characteristic of (σ-B−H) complexes.[3a] The hydride region of the ^1H NMR spectrum of **2** in C_6D_6 at room temperature exhibits two broad signals centered at δ −17.59 and δ −10.20 in a 1:1 integration ratio. The $^1H\{^{11}B\}$ experiment allowed for the detection of the third hydrogen atom as a broad signal at δ 0.76 (Supporting Information, Figure S1). For comparison, in the analogous mesitylborane complex $RuHCl(H_2BMes)(PCy_3)_2$ the corresponding three signals were observed at δ −15.96, δ −7.27, and δ 0.83, respectively. In **2**, the disposition of the hydrogen atoms around the ruthenium center was supported by selective phosphorus and/or boron-decoupled experiments at variable temperature. The resonance at δ −10.20 corresponds to the hydride *cis* to the chloride, whereas the borane is bonded to the ruthenium through two dissymmetrical B−H bonds at a more shielded resonance δ −17.59 for the hydrogen *trans* to Cl and at much lower field (δ 0.76) for the hydrogen *trans* to the hydride, such a difference indicating a different level of bond activation. Additionally, at 223 K, the two nitrogen-bound methyl resonances are resolved at δ 2.39 and δ 2.24 in a 1:1 integration ratio (Supporting Information, Figure S2).

The X-ray structure of **2** was determined at 110 K (Figure 1 and Table 1). The ruthenium atom is in a pseudo-octahedral environment with the phosphines in axial positions (P1−Ru−P2: 164.649(13)°). The coordination sites in the equatorial plane are occupied by one chlorine atom Cl1 and three coplanar hydrogen atoms Hy1, Hy2, and Hy3. Because of the presence of the chlorine atom, it is worth to note the variation of the Ru−B−N angle from 164.7(1)° in **2** to about 180° in the symmetrical dihydrides $RuH_2(\eta^2\text{:}\eta^2\text{-}H_2BNR_2)(PCy_3)_2$ (177.8(2)° for N^iPr_2 and 179.4(2)° for NH_2).[5a,b]

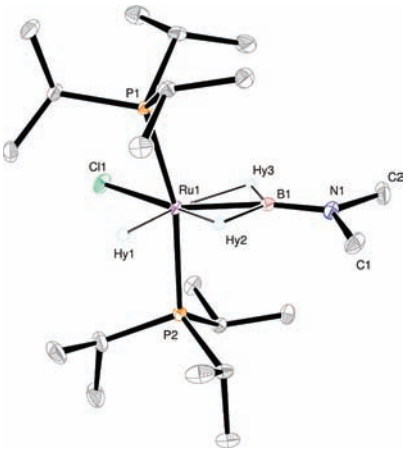

Figure 1. X-ray structure of $RuHCl(H_2BNMe_2)(P^iPr_3)_2$ (**2**). The hydrogen atoms not associated with the metal are omitted for clarity.

Table 1. Selected Geometrical Parameters for the Experimental and Computed Structures of the Ruthenium and Osmium Chloro Complexes 2/2a and 4/4a, Respectively[a]

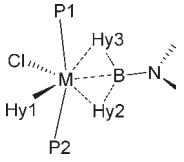

	ruthenium		osmium	
	2	**2a**	**4**	**4a**
M−P1	2.3465(4)	2.343	2.355(1)	2.360
M−P2	2.3566(4)	2.344	2.342(1)	2.360
M−Cl	2.4562(4)	2.455	2.467(1)	2.492
M−Hy1	1.53(2)	1.575	1.59(3)	1.619
M−Hy2	1.58(2)	1.618	1.59(3)	1.616
M···Hy3	1.87(2)	2.000	1.58(4)	1.968
M−B	1.9263(16)	1.924	1.924(7)	1.935
B−Hy3	1.17(2)	1.272	1.22(6)	1.289
B−Hy2	1.53(2)	1.546	1.80(5)	1.946
Hy1−M−Cl	93.8(7)	91.9	91(1)	91.7
Cl−M−B	135.88(5)	137.6	132.8(2)	131.0
Hy1−M−Hy2	79.8(10)	79.6	75(2)	71.6
Hy2−M−B	50.8(7)	50.9	61(1)	65.8
M−B−Hy3	69.4(9)	74.3	55.1(2)	72.1
P1−M−P2	164.649(13)	164.8	166.73(5)	167.4
P2−M−B	91.79(5)	97.5	99.5(2)	96.2
P2−M−Cl	90.886(13)	85.8	86.50(5)	86.5

[a] Distances in Å, angles in degrees.

We prepared the dihydride complex $RuH_2(\eta^2\text{:}\eta^2\text{-}H_2BNMe_2)(P^iPr_3)_2$ (**3**) by stoichiometric addition at room temperature of the lithium dimethylaminoborohydride (Me_2NBH_3Li) to the chloro complex **1** (Scheme 1). Complex **3** was isolated in very good yield as an oil which prevented any X-ray structure determination. **3** was mainly characterized by multinuclear NMR spectroscopy. The $^{11}B\{^1H\}$ NMR spectrum of **3** exhibits a broad signal at δ 48. In the ^1H NMR spectrum two signals were

dx.doi.org/10.1021/ic201573q |*Inorg. Chem.* 2011, 50, 11039–11045

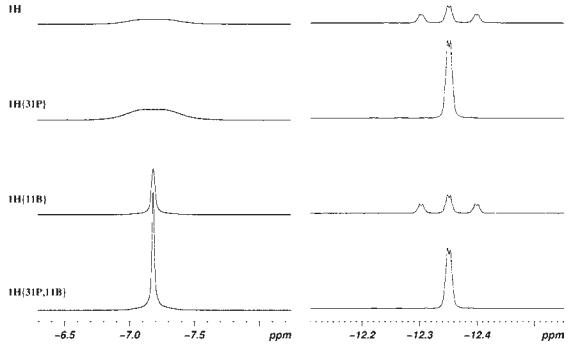

Figure 2. ^{1}H NMR spectra of $RuH_2(H_2BNMe_2)(P^iPr_3)_2$ (**3**) with selective decoupling. From *top* to *bottom*: ^{1}H, ^{1}H{^{31}P}, ^{1}H{^{11}B}, ^{1}H{^{31}P}{^{11}B} spectra in the hydride region.

observed in a 1:1 ratio in the hydride zone: a very broad signal and a triplet of doublets at δ −7.18 and δ −12.35, respectively. As shown in Figure 2, the signal at δ −7.18 is the only one to sharpen upon boron decoupling whereas the other one collapsed into a doublet upon phosphorus decoupling allowing the measurement of a coupling constant value of 2.5 Hz between the two signals (see also Supporting Information, Figures S3 and S4). **3** displays NMR data similar to those reported for the previous series of bis(σ-B−H) ruthenium complexes $RuH_2(\eta^2{:}\eta^2\text{-}H_2BNR_2)(PCy_3)_2$ ($NR_2 = N^iPr_2$, NMe_2, NHMe, NH_2)[5a,b] apart from the coupling between the 2 hydrides and the 2 hydrogen involved in the σ-bond which was never detected.

Computational Study. To gain information on the aminoborane coordination mode at ruthenium and osmium, geometry optimizations of the following species were carried out to model the experimental systems: $RuHCl(H_2BNMe_2)(PMe_3)_2$ (**2a**), $RuH_2(H_2BNMe_2)(PMe_3)_2$ (**3a**), $RuH_2(H_2)_2(PMe_3)_2$ (**5a**), $OsH_2Cl(HBNMe_2)(PMe_3)_2$ (**4a**), and $OsH_2(H_2BNMe_2)(PMe_3)_2$ (**6a**).

The description of the electronic structure of $OsH_2Cl(HBNMe_2)(PMe_3)_2$ (**4a**) as a complex bearing a (σ-B−H) coordinated borinium ligand was very unusual and attracted our attention.[9] The computational proof of the alleged electronic structure resided in a partial analysis of the atomic charges resulting from a Natural Population Analysis (NPA).[10] The osmium charge was computed to be −1.71e,[9] while the boron charge was computed to be +0.66e,[9] and this observation was the only computational evidence to ascertain the borinium nature of the ligand[9] (our computational values were −0.59e and +0.49e, respectively). In itself, it is far from sufficient, as the charge of the whole ligand should have been considered to identify the latter as a borinium $HBNMe_2^+$ moiety. As a matter of fact, we computed the NPA charge of the $HBNMe_2$ entity in **4a** as 0.152e, far from a clearly defined cationic nature. In addition, this is only slightly more positive than the charge for the same group ($HBNMe_2$) in the bis(σ-B−H) ruthenium complex $RuH_2(H_2BNMe_2)(PMe_3)_2$ (**3a**) with a computed NPA charge of 0.061e, while the charge of the entire borane ligand H_2BNMe_2 is 0.057e.

The interaction of the H_2BNMe_2 ligand with the $RuH_2(PMe_3)_2$ fragment in **3a** is clearly defined as a bis(σ-B−H) adduct.[4a,5a,5b] Within the framework of the Natural Bond Orbital (NBO) method, the coordination around a transition metal center is described using six valence orbitals, one s AO and five d AOs.[11] The fragment $RuH_2(PMe_3)_2$ with 14 valence electrons is already hypervalent and the NBO description of this complex leads to three M-L σ-bonds (Ru−H, Ru−H, Ru−P) and one 3c-4e ω-bond involving the two phosphorus atoms and the metal center. The resulting sd^2 hybridation for Ru to create three σ-bonds imposes valence angles of 90° between the ligands, leaving three occupied d AOs as nonbonding lone pair (LP) on ruthenium. The trans geometry for the members of an ω-bonded triad finally completes the overall C_{2v} structure for $RuH_2(PMe_3)_2$. The vacant sites trans to each hydride ligand are available for the creation of two extra ω-bonds with two incoming L ligands leading to a classical 18-electron complex.

A classical example is the bis(dihydrogen) complex $RuH_2(H_2)_2(PR_3)_2$ (**5a** for R = Me) and the coordination of H_2 results from a subtle balance between σ-donation from σ(H−H) to Ru and π-back-donation from a ruthenium d AO to σ^*(H−H). In the realm of NBO analysis, the magnitude of these transfers of electronic density are evaluated using second-order perturbation interaction energies between occupied and vacant NBOs, together with the respective population of these orbitals. An alternative approach is to analyze the composition of the Natural Localized Molecular Orbitals (NLMO) resulting from the aforementioned charge transfers. The advantage of using NLMOs resides in their strict occupation by 2 electrons making thus comparisons between systems more robust. In addition, their composition reflects the result of numerous second-order perturbation energy contributions, thus avoiding the arbitrary choice of isolating a particular one. The NLMO $\underline{\sigma}$(H−H), resulting from the interaction of the NBO σ(H−H) of the H_2 ligand with the metal, is thus expressed as shown in eq 1. The accepting site on the ruthenium is the Ru−H σ^* antibonding orbital (Figure 3). The extent of mixing is thus governed by the electronic influence of the atom bonded trans to H_2. In the same spirit, delocalization of a nonbonding lone pair on ruthenium (LP(Ru)) into the accepting σ^*(H−H) NBO of each H_2 ligand, as illustrated in Figure 3, results in an NLMO $\underline{\text{LP}}$(Ru) as expressed in eq 2. The expression of the two NLMOs indicates that σ-donation from H_2 is stronger than back-donation from the ruthenium atom, as illustrated by the respective weight of the parent NBO in the NLMO (0.925 for σ(H−H) vs 0.960 for LP(Ru)). Consequently, the NPA charge of the H_2 ligand is positive (0.15e).

$$\underline{\sigma}(\text{H-H}) = 0.925\sigma(\text{H-H}) + 0.347\sigma^*(\text{Ru-H}) \quad (1)$$

$$\underline{\text{LP}}(\text{Ru}) = 0.960\text{LP}(\text{Ru}) - 0.194\sigma_1^*(\text{H-H}) - 0.194\sigma_2^*(\text{H-H}) \quad (2)$$

In the case of the adduct between $RuH_2(PMe_3)_2$ and H_2BNMe_2 to form **3a**, the NBO analysis yielded a Lewis structure qualitatively similar to that for **5a** (Figure 4). Donation from the occupied σ(B−H) NBO into σ^*(Ru−H) corresponds to σ-donation from the borane ligand, and the resulting NLMO (see Table 2) indicates that σ-donation from the borane ligand is weaker than from an H_2 ligand. Back-donation from $d_{x^2-y^2}$ ($LP_{x^2-y^2}$(Ru)) into the antibonding σ^*(B−H) NBOs is also weaker than the corresponding transfer in **5a**, as illustrated by the composition of the NLMO (Table 2). However, in the case of **3a**, an additional interaction between an occupied lone pair on ruthenium (LP_{xz}(Ru)) and a vacant orbital on the borane ligand (π^*(B−N)) contributes to an increase of the interaction between the ruthenium and the borane ligand. This additional charge transfer from the metal to the ligand compensates for the donation from the ligand to the metal and overall the

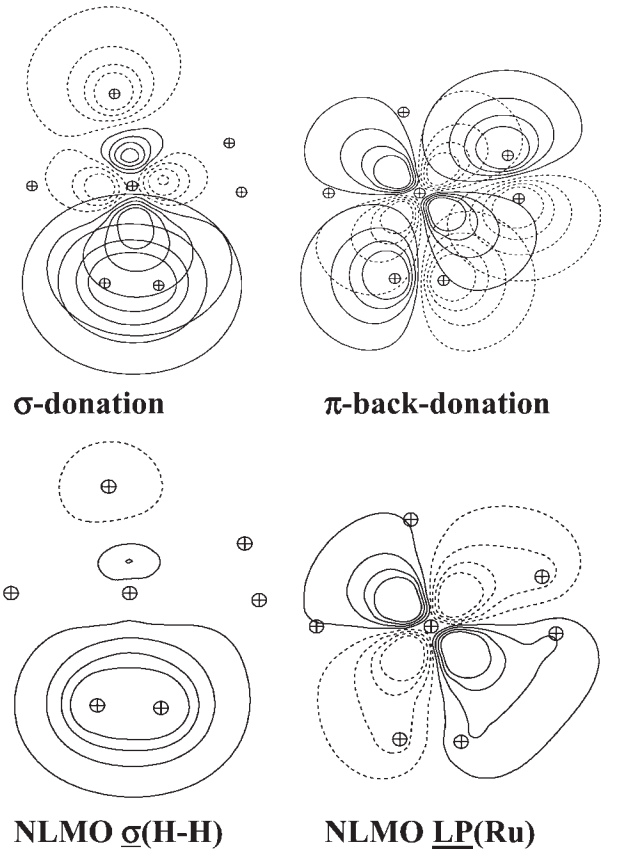

Figure 3. Overlap (top) between the two NBOs involved in the charge transfers between H_2 and Ru and the resulting NLMO (bottom). Contour plots in the equatorial plane containing the hydrogen atoms are represented.

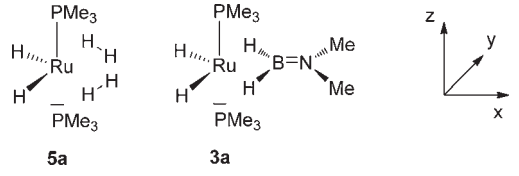

Figure 4. Lewis structures obtained from a NBO analysis of the ruthenium dihydride species **3a** and **5a**.

latter is barely positively charged (0.057e). Calculations on the osmium bis(σ-B−H) complex $OsH_2(PMe_3)_2(H_2BNMe_2)$, **6a**, yielded similar results. The expression of the NLMOs are indicative of slightly larger both σ-accepting and π-donating capacities of the $OsH_2(PMe_3)_2$ fragment (Table 2). However, as in the ruthenium case, these synergetic charge transfers result in a barely positively charged borane ligand (0.063e).

The symmetric coordination of the two B−H bonds to $MH_2(PMe_3)_2$ (M = Ru, Os) is necessarily altered when a hydride is substituted by a chloride as in $MHCl(PMe_3)_2$. The electronegative nature of chloride compared to hydride results in a σ(M-Cl) bond strongly developed on Cl and at a lower energy than σ(M-H). Concomitantly, the σ-accepting ability of σ*(M-Cl) is increased compared to σ*(M-H) because the antibonding orbital is more strongly developed on the metal (better overlap) and its energy is lower (i.e., there is a lower energy gap between it and the donating NBO). The σ-donation from the B−H bond trans

Table 2. Composition of the NLMOs Involved in the σ-Donation and π-Back-Donation Charge Transfer Processes in the Ruthenium (2a, 3a, 5a) and Osmium (4a, 6a) Complexes

2a

$\underline{\sigma}(B-H) = 0.959\ \sigma(B-H) - 0.256\ \sigma^*(Ru-H)$

$\underline{LP}_{xz}(Ru) = 0.948\ LP_{xz}(Ru) - 0.276\ \pi^*(B-N)$

$\underline{LP}_{x^2-y^2}(Ru) = 0.957\ LP_{x^2-y^2}(Ru) + 0.162\ LP(H) - 0.187\ LP^*(B) - 0.113\ \sigma^*(B-H)$

$\underline{LP}(H) = 0.644\ LP(H) + 0.556\ LP^*(B) + 0.478\ \sigma^*(Ru-Cl)$

3a

$\underline{\sigma}(B-H) = 0.937\ \sigma(B-H) + 0.321\ \sigma^*(Ru-H)$

$\underline{LP}_{xz}(Ru) = 0.939\ LP_{xz}(Ru) - 0.292\ \pi^*(B-N)$

$\underline{LP}_{x^2-y^2}(Ru) = 0.974\ LP_{x^2-y^2}(Ru) - 0.136\ \sigma_1^*(B-H) - 0.136\ \sigma_2^*(B-H)$

4a

$\underline{\sigma}(B-H) = 0.940\ \sigma(B-H) - 0.309\ \sigma^*(Os-H)$

$\underline{LP}_{xz}(Ru) = 0.941\ LP_{xz}(Ru) - 0.289\ \pi^*(B-N)$

$\underline{LP}(H) = 0.674\ LP(H) + 0.439\ LP^*(B) - 0.554\ \sigma^*(Os-Cl)$

5a

$\underline{\sigma}(H-H) = 0.925\ \sigma(H-H) + 0.347\ \sigma^*(Ru-H)$

$\underline{LP}_{x^2-y^2}(Ru) = 0.960\ LP_{x^2-y^2}(Ru) - 0.194\ \sigma_1^*(H-H) - 0.194\ \sigma_2^*(H-H)$

6a

$\underline{\sigma}(B-H) = 0.924\ \sigma(B-H) + 0.355\ \sigma^*(Os-H)$

$\underline{LP}_{xz}(Os) = 0.927\ LP_{xz}(Os) - 0.321\ \pi^*(B-N)$

$\underline{LP}_{x^2-y^2}(Os) = 0.962\ LP_{x^2-y^2}(Os) - 0.175\ \sigma_1^*(B-H) - 0.175\ \sigma_2^*(B-H)$

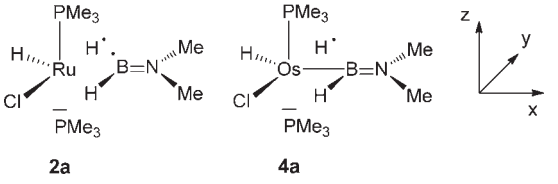

Figure 5. Lewis structures obtained from an NBO analysis of the chloro complexes **2a** (Ru) and **4a** (Os).

to Cl is thus expected to be stronger than that trans to the hydride, to such an extent that breaking of the B−H bond could be observed. This is indeed what is observed experimentally in **2** and **4** with long Hy2···B distances (1.53(2) Å, **2**; 1.80(5) Å, **4**). The computed geometries for the model complexes (PMe_3 instead of P^iPr_3) are in very good agreement with the experimental structures (see Supporting Information). The calculated values for the Hy2···B distances are indicative of strongly reduced (1.546 Å, **2a**) or absent (1.946 Å, **4a**) bonding interaction between the two atoms. Both experimentally and computationally, there is a significant difference in the degree of activation of the B−H bond trans to Cl between ruthenium and osmium. In the case of the ruthenium species **2a**, the B···H bond is stretched but still within bonding interaction regime. In the case of the osmium species **4a**, the B···H distance is too long to invoke any bonding interaction. This difference is also reflected in the NBO description of the electronic structure of the two species.

The NBO procedure for **2a** yielded a Lewis structure typical of a ruthenium(II) complex with three d lone pairs on ruthenium and three σ-bonds (Figure 5). The B−H bond trans to Cl is broken and the NBO procedure yielded two "singly" occupied

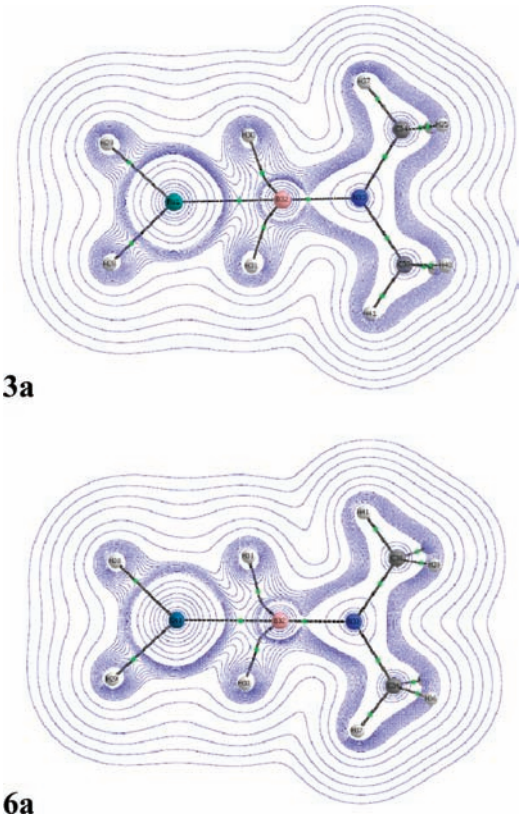

Figure 6. Contour plot of the electron density in the equatorial plane of the dihydrides **3a** (Ru) and **6a** (Os) with the molecular graph showing the bond paths (black lines) and bond critical points (green dots).

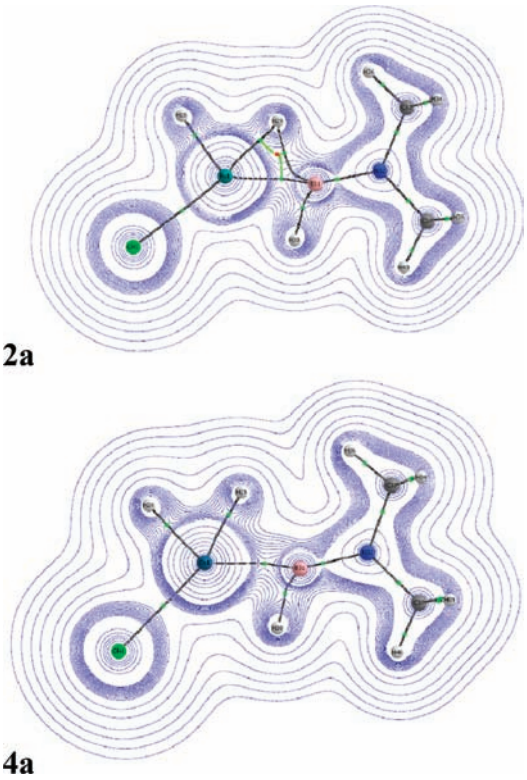

Figure 7. Contour plot of the electron density in the equatorial plane of the chloro complexes **2a** (Ru) and **4a** (Os) with the molecular graph showing the bond paths (black lines), bond critical points (green dots), and ring critical point (red dot) in the case of **2a**.

NBOs located respectively on H (LP(H), 0.91e) and B (LP*(B), 0.72e, hybridization $sp^{2.86}$). The expression of the NLMOs still identifies the σ-donation from the B−H bond trans to the hydride and the back-donation from the d_{xz} lone pair on ruthenium into π^*(B−N) (Table 2). σ-donation from the B···H bond trans to Cl is apparent in the expression of the NLMO for the s lone pair on H, which is strongly delocalized onto both the ruthenium and the boron atoms. The large weight on σ^*(Ru−Cl) clearly indicates a strong participation of this component and hence a significant H···Ru bonding interaction. Back-donation from $LP_{x^2-y^2}$(Ru) into σ^*(B−H) also involves contributions from LP(H) and LP*(B), thus recovering somehow the antibond associated to the stretched B−H bond (Table 2). The NBO description of the ruthenium **2a** is thus that of a bis(σ-B−H) borane adduct with a stretched B···H bond trans to Cl. The latter sets the bridging hydrogen atom in strong interaction with both Ru and B.

The NBO analysis of the electronic structure of the osmium **4a** yielded a significantly different result (Figure 5). In that case, the activation of the B−H bond trans to Cl is strong enough to result in complete breaking of the bond. The Lewis structure is typical of an Os(IV) complex with four σ-bonds (Os−H, Os−Cl, Os−P, Os−B) and two occupied d AOs lone pair on Os. The hydrogen atom, initially bonded to B, is described by a s lone pair (LP(H)) occupied by 0.937e. There is still σ-donation from the remaining B−H bond and back-donation from LP_{xz}(Os) into π^*(B−N) as illustrated by the composition of the corresponding NLMOs (Table 2). As in the case of ruthenium, the NBO LP(H) is strongly interacting with accepting NBOs on the metal (σ^*(Os−Cl)) and on the boron atom (σ^*(B−H)). The composition of the resulting NLMO indicates a stronger contribution of the component centered on the metal. There is thus a significantly stronger bonding interaction with osmium and the complex is better described as an osmium(IV) hydrido-boryl complex with an α-agostic interaction of the boryl B−H bond.

To ascertain the differences in the description of the electronic structures of **2a** and **4a** as obtained from the NBO method, an Atom in Molecule (AIM) analysis of the topology of the electron density was carried out.[12] AIM has been recently used by Stradiotto to probe the ligation of mesitylborane to the cationic fragment $Cp^*Ru(P^iPr_3)^+$.[13] The bis(σ-B−H) coordination of the borane was evidenced, and the description was complementary to that obtained from NBO. Figure 6 shows a contour plot of the density in the equatorial plane for the dihydrides **3a** and **6a**. The bond critical point (bcp) between M and B is the result of the back-donation from the metal to boron as illustrated by the values of the ellipticity at these bcp (ε = 0.465, M = Ru; ε = 0.257, M = Os). The presence of a bcp between B and H confirms the bonding interaction between these atoms.[14] The curvature of the bond path for B−H originates from the transfer of density from this bond to the metal, even though there is no explicit bcp between H and the metal.

The same type of analysis was carried out for the chloro complexes **2a** and **4a**, and the contour plots of the density in the equatorial plane are shown in Figure 7. The main difference between the molecular graphs is the topology around the hydrogen atom trans to Cl. In **2a**, the bcp between H and B is still present but, in addition, there is now a bcp between H and Ru indicative of a developing bonding interaction between the two

dx.doi.org/10.1021/ic201573q |*Inorg. Chem.* 2011, 50, 11039–11045

atoms. The AIM analysis is thus in agreement with the description of **2a** as a bis(σ-B−H) borane adduct with a stretched B···H bond featuring a strong H···Ru interaction. In the osmium case, the AIM analysis highlights the complete breaking of any bonding interaction between H and B for the hydrogen trans to Cl. The topology of the density is thus in agreement with the description of the complex as an Os(IV) hydrido-boryl species.

CONCLUSION

In a previous communication, we had found a novel access to a neutral borylene species by adding mesitylborane to the ruthenium precursor **1**.[6] This reaction occurred via the intermediacy of $RuHCl(H_2BMes)(PCy_3)_2$, a compound formulated as a bis(σ-B−H) species on the basis of NMR data. Herein, the isolation of the hydrido(chloro) complex $RuHCl(H_2BNMe_2)(P^iPr_3)_2$ (**2**) featuring a dimethylaminoborane ligand, and its characterization by a variety of techniques, including X-ray diffraction, supports such a formulation and shows that substituent effects are key parameters in this area. Indeed, **2** proved to be very stable under vacuum, and under standard conditions, we were not able to generate a borylene species.

Ruthenium chemistry is dominated by the formation of bis(σ-B−H) species either symmetrical in the case of the dihydrides or unsymmetrical in the case of the chloro(hydrido) compounds. In the latter system, the two σ-B−H bonds display rather different levels of activation as evidenced by several parameters (NMR chemical shifts, X-ray distances and angles, NBO and particularly AIM analyses). In contrast, in the osmium case, introduction of the chloride in the metal coordination sphere pushes the B−H activation up to the point of breaking, and the corresponding complex resulting from oxidative addition of the borane can be isolated. This follows the usual trend observed for these two metals: σ-bonding preferred at ruthenium versus oxidative addition at osmium. As opposed to the surprising borinium formulation initially published for $OsH_2Cl(HBNMe_2)(P^iPr_3)_2$ (**4**), we thus propose a dihydride(boryl)(chloro) osmium(IV) formulation with an α-agostic B−H interaction. Our in-depth theoretical analysis allows to better define the differences between analogous ruthenium and osmium species and to emphasize the difficulties in assigning bonding modes in the continuum of the B−H bond activation process.[15]

EXPERIMENTAL SECTION

General Considerations. All reactions were carried out under an argon atmosphere using either Schlenk tube or glovebox techniques. Diethylether, pentane, and toluene were obtained from a solvent purification system MBraun SPS-800 Series. Deuterated NMR solvents were dried over activate 4 Å molecular sieves, degassed by freeze−pump−thaw cycles, and stored under argon. NMR samples of sensitive compounds were prepared in the glovebox using NMR tubes fitted with Teflon septa. $RuH(\eta^2\text{-}H_2)Cl(P^iPr_3)_2$ was prepared according to literature procedures.[16] Dimethylamine borane ($Me_2NH\text{-}BH_3$) was purchased from Aldrich and used as received. NMR spectra were recorded on Bruker AV 300 (^{1}H 300.13 MHz, ^{31}P 121.5 MHz, ^{13}C 75 MHz), 400 (^{1}H 400.13 MHz, ^{31}P 162 MHz, ^{13}C 100 MHz, ^{11}B 128.38 MHz), or 500 (^{1}H 500.33 MHz, ^{31}P 202.5 MHz, ^{13}C 125 MHz, ^{11}B 160.53 MHz) spectrometers. ^{1}H and ^{13}C chemical shifts are reported in ppm referenced internally to residual protio-solvent, ^{31}P and ^{11}B relative to a 85% H_3PO_4 and $BF_3.OEt_2$ external references, respectively. Chemical shifts are quoted in δ (ppm) and coupling constants in hertz. Elemental analyses were performed by the "in house" service of the Laboratoire de Chimie de Coordination, Toulouse.

Synthesis of $[Me_2NBH_2]_2$. Dimethylamine borane (5 g, 84.861 mmol) was heated neat under an argon atmosphere at 403 K in a trap-to-trap distillation apparatus connected to a mineral oil containing bubbler with the receiving Schlenk tube in an ethanol/liquid nitrogen cooling bath (−78 °C). Heating was prolonged until dihydrogen evolution ceased. Dimethylaminoborane dimer was quantitatively obtained as a shiny crystalline compound.

$^1H\{^{11}B\}$ NMR (400 MHz, C_7D_8, 298 K): δ 2.98 (s, 4H, BH_2), 2.27 (s, 12H, Me); ^{11}B (128.38 MHz, C_7D_8, 25 °C) δ 5.53 (t, $^1J_{BH}$ = 113 Hz).

Synthesis of $RuHCl(H_2BNMe_2)(P^iPr_3)_2$ (2). A toluene solution (5 mL) of $RuH(\eta^2\text{-}H_2)Cl(P^iPr_3)_2$ (200 mg, 0.43 mmol) was stirred in the presence of an excess of dimethylaminoborane dimer (173 mg, 3.0 mmol) during 18 h. The solvent was evaporated, and pentane (3 mL) was added. The supernatant was eliminated. The resulting yellow solid was washed twice with a minimum amount of pentane and dried under vacuum (155 mg, 69%). X-ray diffraction quality crystals were obtained by recrystallization in pentane at −40 °C under an argon atmosphere. $^1H\{^{11}B\}$ NMR (500.130 MHz, C_7D_8, 193 K): δ −17.75 (bs, 1H, Ru*H* (trans to Cl)), −10.01 (td, 1H, $^2J_{HH}$ = $^2J_{PH}$ = 16 Hz, Ru*H*B (cis to Cl)), 0.45 (bs, 1H, Ru*H*B (cis to Cl)), 1.31 (m, 36H, C*H*$_3$ P(^{i}Pr)$_3$), 2.18 and 2.37 (s, 2 × 3H, NMe_2), 2.27 (bs, 6H, C*H* P(^{i}Pr)$_3$); $^{13}C\{^1H,^{31}P\}$-(125.808 MHz, C_7D_8, 298 K) 19.73, 20.05 (s, *C*H$_3$ P(^{i}Pr)$_3$), 25.39 (s, *C*H P(^{i}Pr)$_3$), 38.74 and 38.81 (s, N(*C*H$_3$)$_2$) ; $^{31}P\{^1H\}$(161.976 MHz, C_6D_6, 298 K) 64.6 (s); $^{11}B\{^1H\}$(128.377 MHz, C_6D_6, 298 K) 56 (bs). Anal.Calcd for $C_{20}H_{51}NBP_2RuCl$: C, 46.65; H, 9.98; N, 2.72. Found: C, 46.73; H, 10.04; N, 2.82. IR (neat): ν = 2066 and 2036 (m br) cm^{-1}.

Synthesis of $RuH_2(\eta^2\text{:}\eta^2\text{-}H_2BNMe_2)(P^iPr_3)_2$ (3). An ethereal solution (2 mL) of lithium dimethylaminoborohydride.0.33 pentane (19.3 mg, 0.217 mmol) was added to a diethylether solution (2 mL) of $RuHCl(\eta^2\text{-}H_2)(P^iPr_3)_2$ (100 mg, 0.217 mmol) at room temperature, and the solution stirred during 15 min. The solvent was evaporated under vacuum and toluene (4 mL) was added. After filtration over activated Celite, the filtrate was evaporated under vacuum and compound **3** was obtained as a brown oil (101 mg, 97%). ^{1}H (500.330 MHz, C_7D_8, 298 K) δ 2.62 (s, 6H, NMe_2), 1.93 (sept d, 6H, $^3J_{HH}$ = 7 Hz, J_{PH}= 13 Hz, C*H* P(^{i}Pr)$_3$), 1.25 (dt, 36H, $^3J_{HH}$ = 7 Hz, J_{PH}= 7 Hz, C*H*$_3$ P(^{i}Pr)$_3$), −7.18 (bs, 2H, BH_2, $T_{1\ min}$(208 K, 167 ms)), −12.35 (td, 2H, $^2J_{PH}$ = 24.15 Hz, $^2J_{HH}$ = 2.4 Hz, RuH_2, $T_{1\ min}$(213 K, 424 ms)); $^{13}C\{^1H\}$(100.612 MHz, C_6D_6, 298 K) δ 39.27 (s, NMe_2), 27.80 (m, CH P(^{i}Pr)$_3$), 20.60 (s, *C*H$_3$ P(^{i}Pr)$_3$); $^{31}P\{^1H\}$(161.975 MHz, C_7D_8, 298 K) δ 90.5 (s); $^{11}B\{^1H\}$ (128.38 MHz, C_7D_8, 298 K) δ 48 (bs). IR (neat): ν = 1941 and 1902 (m br, RuH) cm^{-1}.

Computational Details. All the calculations have been performed with the Gaussian09 package at the B3PW91 level.[17] For the optimization of geometry, the ruthenium and osmium atoms were represented by the relativistic effective core potential (RECP) from the Stuttgart group and the associated basis sets,[18] augmented by an f polarization function.[19] The phosphorus and chlorine atoms were represented by a RECP from the Stuttgart group and the associated basis set,[20] augmented by a d polarization function.[21] The remaining atoms (C, H, N, B) were represented by a 6-31G(d,p) basis set. The NBO and AIM analyses were performed on electron densities computed on the optimized geometries with the same basis set for Ru and Os, but with a 6-311G(d,p) basis set for the remaining atoms. The NBO analyses were performed with NBO 5.9 interfaced with Gaussian09, and the AIM analyses were carried out by the AIMALL software developed by T. A. Keith at http://aim.tkgristmill.com/.

ASSOCIATED CONTENT

Supporting Information. Crystal structural data for compound **2** in CIF format. NMR spectra for compounds **2** and **3**.

dx.doi.org/10.1021/ic201573q |Inorg. Chem. 2011, 50, 11039–11045

Coordinates for the calculated structures and full citation for ref 17a. This material is available free of charge via the Internet at http://pubs.acs.org.

AUTHOR INFORMATION

Corresponding Author

*E-mail: gilles.alcaraz@lcc-toulouse.fr (G.A.), clot@univ-montp2.fr (E.C.), sylviane.sabo@lcc-toulouse.fr (S.S.-E.).

ACKNOWLEDGMENT

We thank the CNRS and the ANR for support through the HyBoCat ANR-09-BLAN-0184 program. G.B.-L. thanks the DGA for financial support. Johnson Matthey is gratefully acknowledged for a generous loan of $RuCl_3 \cdot nH_2O$. The authors also thank Prof. Miguel-Angel Esteruelas and Dr. Ana López for fruitful discussions within the PICASSO PHC program.

REFERENCES

(1) (a) Irvine, G. J.; Lesley, M. J. G.; Marder, T. B.; Norman, N. C.; Rice, C. R.; Robins, E. G.; Roper, W. R.; Whittell, G. R.; Wright, L. J. *Chem. Rev.* **1998**, *98*, 2685–2722. (b) Dang, L.; Lin, Z.; Marder, T. B. *Chem.Commun.* **2009**, 3987–3995. (c) Braunschweig, H.; Dewhurst, R. D.; Schneider, A. *Chem. Rev.* **2010**, *110*, 3924–3957. (d) Hamilton, C. W.; Baker, R. T.; Staubitz, A.; Manners, I. *Chem. Soc. Rev.* **2009**, *38*, 279–293. (e) Staubitz, A.; Robertson, A. P. M.; Manners, I. *Chem. Rev.* **2010**, *110*, 4079–4124. (f) Staubitz, A.; Robertson, A. P. M.; Sloan, M. E.; Manners, I. *Chem. Rev.* **2010**, *110*, 4023–4078. (g) Crudden, C. M.; Glasspoole, B. W.; Lata, C. J. *Chem.Commun.* **2009**, 6704–6716. (h) Vidovic, D.; Pierce, G. A.; Aldridge, S. *Chem. Commun.* **2009**, 1157–1171. (i) Mkhalid, I. A. I.; Barnard, J. H.; Marder, T. B.; Murphy, J. M.; Hartwig, J. F. *Chem. Rev.* **2009**, *110*, 890–931.

(2) Hartwig, J. F.; Muhoro, C. N.; He, X.; Eisenstein, O.; Bosque, R.; Maseras, F. *J. Am. Chem. Soc.* **1996**, *118*, 10936–10937.

(3) (a) Alcaraz, G.; Sabo-Etienne, S. *Coord. Chem. Rev.* **2008**, *252*, 2395–2409.(b) Kubas, G. J. *Metal Dihydrogen and sigma-Bond Complexes*; Kluwer Academic/Plenum Publishers: New York, 2001.

(4) (a) Alcaraz, G.; Clot, E.; Helmstedt, U.; Vendier, L.; Sabo-Etienne, S. *J. Am. Chem. Soc.* **2007**, *129*, 8704–8705. (b) Alcaraz, G.; Grellier, M.; Sabo-Etienne, S. *Acc. Chem. Res.* **2009**, *42*, 1640–1649.

(5) (a) Alcaraz, G.; Vendier, L.; Clot, E.; Sabo-Etienne, S. *Angew. Chem., Int. Ed.* **2010**, *49*, 918–920. (b) Alcaraz, G.; Chaplin, A. B.; Stevens, C. J.; Clot, E.; Vendier, L.; Weller, A. S.; Sabo-Etienne, S. *Organometallics* **2010**, *29*, 5591–5595. (c) Stevens, C. J.; Dallanegra, R.; Chaplin, A. B.; Weller, A. S.; Macgregor, S. A.; Ward, B.; McKay, D.; Alcaraz, G.; Sabo-Etienne, S. *Chem.—Eur. J.* **2011**, *17*, 3011–3020. (d) Tang, C. Y.; Thompson, A. L.; Aldridge, S. *Angew. Chem., Int. Ed.* **2010**, *49*, 921–925.

(6) Alcaraz, G.; Helmstedt, U.; Clot, E.; Vendier, L.; Sabo-Etienne, S. *J. Am. Chem. Soc.* **2008**, *130*, 12878–12879.

(7) Vidovic, D.; Addy, D. A.; Krämer, T.; McGrady, J.; Aldridge, S. *J. Am. Chem. Soc.* **2011**, *133*, 8494–8497.

(8) O'Neill, M.; A. Addy, D.; Riddlestone, I.; Kelly, M.; Phillips, N.; Aldridge, S. *J. Am. Chem. Soc.* **2011**, *133*, 11500–11503.

(9) Esteruelas, M. A.; Fernández-Alvarez, F. J.; López, A. M.; Mora, M.; Oñate, E. *J. Am. Chem. Soc.* **2010**, *132*, 5600–5601.

(10) Reed, A. E.; Weinstock, R. B.; Weinhold, F. *J. Chem. Phys.* **1985**, *83*, 735–746.

(11) (a) Reed, A. E.; Curtiss, L. A.; Weinhold, F. *Chem. Rev.* **1988**, *88*, 899–926.(b) Weinhold, F.; Landis, C. R. *Valency and Bonding: A Natural Bond Orbital Donor-Acceptor Perspective*; Cambridge University Press: Cambridge, U.K., 2005.

(12) Bader, R. F. W. *Atoms in Molecules, A Quantum Theory*; Oxford University Press: Oxford, U.K., 1990.

(13) Hesp, K. D.; Kannemann, F. O.; Rankin, M. A.; McDonald, R.; Ferguson, M. J.; Stradiotto, M. *Inorg. Chem.* **2011**, *50*, 2431–2444.

(14) (a) Cortés-Guzmán, F.; Bader, R. F. W. *Coord. Chem. Rev.* **2005**, *249*, 633–662. (b) Bader, R. F. W. *J. Phys. Chem. A* **2009**, *113*, 10391–10396. (c) Bader, R. F. W. *J. Phys. Chem. A* **2010**, *114*, 7431–7444.

(15) Demachy, I.; Esteruelas, M. A.; Jean, Y.; Lledós, A.; Maseras, F.; Oro, L. A.; Valero, C.; Volatron, F. *J. Am. Chem. Soc.* **1996**, *118*, 8388–8394.

(16) Wolf, J.; Stüer, W.; Grünwald, C.; Gevert, O.; Laubender, M.; Werner, H. *Eur. J. Inorg. Chem.* **1998**, 1827–1834.

(17) (a) Frisch, M. J. T. et al. *Gaussian 09*, Revision B.1; Gaussian Inc.: Wallingford, CT, 2009. (b) Becke, A. D. *J. Chem. Phys.* **1993**, *98*, 5648–5652. (c) Perdew, J. P.; Wang, Y. *Phys. Rev. B* **1992**, *45*, 13244–13249.

(18) Andrae, D.; Häussermann, U.; Dolg, M.; Stoll, H.; Preuss, H. *Theor. Chim. Acta* **1990**, *77*, 123–141.

(19) Ehlers, A. W.; Böhme, M.; Dapprich, S.; Gobbi, A.; Höllwarth, A.; Jonas, V.; Köhler, K. F.; Stegmann, R.; Veldkamp, A.; Frenking, G. *Chem. Phys. Lett.* **1993**, *208*, 111–114.

(20) Bergner, A.; Dolg, M.; Kuchle, W.; Stoll, H.; Preuss, H. *Mol. Phys.* **1993**, *80*, 1431–1441.

(21) Höllwarth, A.; Böhme, H.; Dapprich, S.; Ehlers, A. W.; Gobbi, A.; Jonas, V.; Köhler, K. F.; Stegmann, R.; Veldkamp, A.; Frenking, G. *Chem. Phys. Lett.* **1993**, *208*, 237–240.